Available online at www.sciencedirect.com
SCIENCE DIRECT
Trans. Nonferrous Met. Soc. China 17(2007) 468−473
Transactions of Nonferrous Metals Society of China
www.csu.edu.cn/ysxb/

Processing and mechanical properties of porous 316L stainless steel for biomedical applications

Montasser M. DEWIDAR[1, 2], Khalil A. KHALIL[1], J. K. LIM[3]

1. Department of Mechanical Design and Materials, High Institute of Energy, South Valley University, Aswan, Egypt;
2. Material and Fracture Laboratory, Department of Mechanical Design, Chonbuk National University, Duckjin 1-664-14, Jeonju, JB561-756, South Korea;
3. Automobile Hi-Technology Research Institute, Faculty of Mechanical and Aerospace System Engineering, Chonbuk National University, Duckjin 1-664-14, Jeonju, JB 561-756, South Korea

Received 21 September 2006; accepted 26 January 2007

Abstract: Highly porous 316L stainless steel parts were produced by using a powder metallurgy process, which includes the selective laser sintering(SLS) and traditional sintering. Porous 316L stainless steel suitable for medical applications was successfully fabricated in the porosity range of 40%−50% (volume fraction) by controlling the SLS parameters and sintering behaviour. The porosity of the sintered compacts was investigated as a function of the SLS parameters and the furnace cycle. Compressive stress and elastic modulus of the 316L stainless steel material were determined. The compressive strength was found to be ranging from 21 to 32 MPa and corresponding elastic modulus ranging from 26 to 43 GPa. The present parts are promising for biomedical applications since the optimal porosity of implant materials for ingrowths of new-bone tissues is in the range of 20%−59% (volume fraction) and mechanical properties are matching with human bone.

Key words: 316L stainless steel; laser sintering; processing parameter; porous material; biomedical application

1 Introduction

Despite the great progress that has been achieved in orthopedic biomaterials, fixation of implants to the bone host remains a problem. Mismatch of elastic moduli of the biomaterials and the surrounding bone has been identified as a major reason for implant loosening following stress shielding of bone. However, the implanted material must be strong enough and durable to withstand the physiological loads placed upon it over the years. The elastic modulus of natural bone is ranging from 10 to 30 GPa[1], which is much lower than that of artificial bone made by 316L stainless steel. One way to alleviate these problems is to reduce modulus of elasticity of metallic materials by introducing pores, thereby minimizing damages to tissues adjacent to the implant and eventually prolong device lifetime[2−3]. A porous implant material with adequate pore structure and appropriate mechanical properties has been sought as the ideal bone substitute. Furthermore, porous components based on biocompatible metallic materials are expected to provide better interaction with bones[4]. The main advantage of porous materials is their ability to provide biological anchorage for the surrounding bony tissue via the ingrowth of mineralized tissue into the pore space and allow body fluids to be transported through the interconnected pores[5−8]. 316L stainless steel is considered as one of the attractive metallic materials for biomedical applications due to its mechanical properties, biocompatibility, and corrosion resistance. This material is popular metal for use as acetabula cup (one half of an artificial hip joint) applications. This popularity stems from a satisfactory combination of good mechanical properties and reasonable cost. In sintered porous materials mechanical properties are dependent on two essential parameters: 1) the size of the interparticle necks which determines the amount load bearing area available; 2) the stress distribution around the pores, where the level of stress concentration is dependent on the pores geometry i.e. size and shape. Higher stress concentration factors would be expected with small pores of a highly

Corresponding author: J. K. LIM; E-mail: jklim@chonbuk.ac.kr

irregular shape[9−11]. Therefore, a large amount of experimental work has been carried out with porous materials, to determine the elastic/plastic properties, the fatigue life and fracture toughness[12−14]. Conducted predominantly on sintered iron and steel the majority of mechanical properties for powder metallurgy produced porous materials have been found to be largely dependent on the amount of total porosity[15−16].

On the other hand, selective laser sintering(SLS) is a new direction of manufacturing to produce parts directly from metal powders. It is advanced technique for producing components from various powder materials with complicated spatial forms. The laser sintering is very complicated process, and several parameters influence the densification mechanism. Laser power (P), scan speed (v), scan spacing (h), thickness of layer (d), and powder bed temperature are the main parameters. In this experimental study, the effects of processing parameters of selective laser sintering and sintering furnace on the mechanical properties of 316L stainless steel parts were investigated. The mechanical properties of porous 316L stainless steel that can potentially be used in biomedical applications were achieved using selective laser sintering process and subsequent traditional sintering process. The fabricated parts were characterized by scanning electron microscopy.

2 Experimental

Gas atomized 316L stainless steel powders with mean particle size 40 μm coated with 2%−3% (mass fraction) of mixture of thermoplastic resin mixture (e.g. wax and phenolic) was used for this investigation. The 316L stainless steel powder was supplied by DTM Corp., USA. Selective laser sintering of the as supplied 316L stainless steel powders was performed using the DTM Sinterstation 2000. The selective laser sintering process is illustrated in Fig.1. A bed of the powder was heated under the action of a laser beam. The laser was used to heat the polymer binder to a temperature above its activation temperature, producing a green part in which the particles were bonded together by polymer-polymer bonds. By directing the laser only to those areas where binding was required a thin cross-section of green part could be generated. When the first thin cross section was complete the powder bed was lowered, and a layer of virgin powder was deposited on top of this layer. A second layer was then generated through the action of the laser which adhered to the layer below. This process continued until the series of layers completed, which generated the required geometry. At this stage the required geometry was surrounded by powder which has not been scanned by the laser. To allow access to the component the piston rose, loose powder from around the component was swept away and the required geometry removed. Further excess powder was removed using a brush. Fig.2 shows a schematic diagram of the three stages of production of porous parts. This process was used for the production of any complicated shapes. Five samples with diameter of 10 mm, and height of 10 mm were manufactured, for each processing parameters, according to the conditions listed in Table 1. The green specimens were sintered in a vacuum furnace (p=10^{-3} Pa). The sintering temperature of all samples was 1 150 ℃ for 2 h which recommended by DTM[17]. Compressive testing of all specimens was conducted using

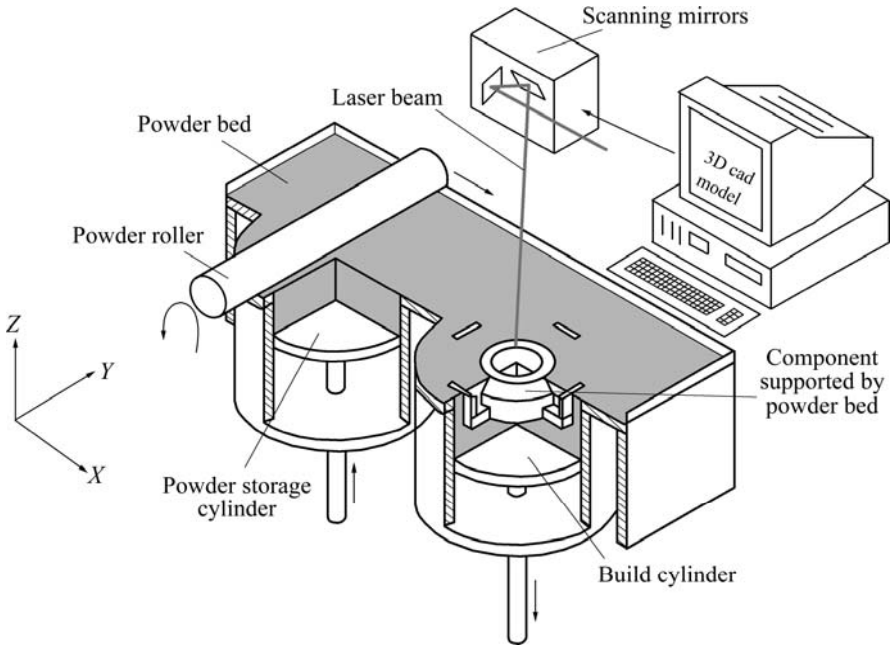

Fig.1 Schematic diagram of selective laser sintering process

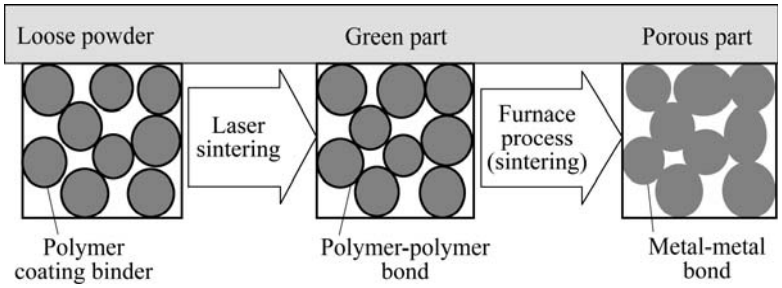

Fig.2 Stages of production of porous 316L stainless steel material

Table 1 Processing parameters of selective laser sintering

Item	Condition
Laser powder (P)	15−30 W, 5 W/step
Scan speed (v)	900−1 500 mm/s, 200 mm/step
Scan spacing (h)	0.08−0.24 mm, 0.04 mm/step
Powder layer thickness (d)	0.075 mm
Part bed temperature	120 ℃

universal testing machine at a fixed cross-head speed of 0.05 mm/s. The microstructures were examined using scanning electron microscopy(SEM).

3 Results and discussion

3.1 Selective laser sintering processing parameters

Fig.3 shows SEM micrograph of as supplied starting materials of resin coated 316L stainless steel powder particles. The 316L stainless steel powder is entirely spherical in shape. The average particle size of the powder is 40 μm.

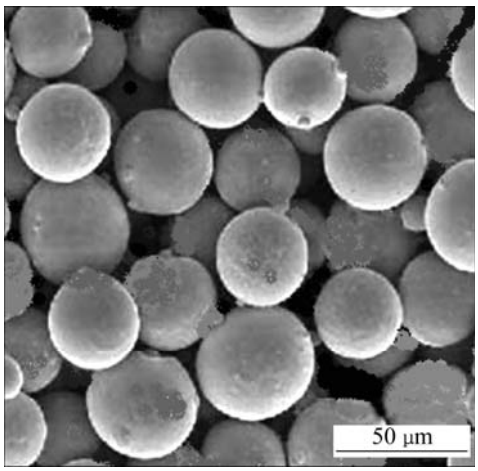

Fig.3 SEM micrograph of loose 316L stainless steel powders

Figs.4, and 5 show the effect of SLS processing parameters on the porosity of the investigated 316L stainless steel powder. At constant laser power (P=20 W), and different scan spacing, an increase in scan speed increases the porosity (Fig.4(a)). Fig.4(b) shows the

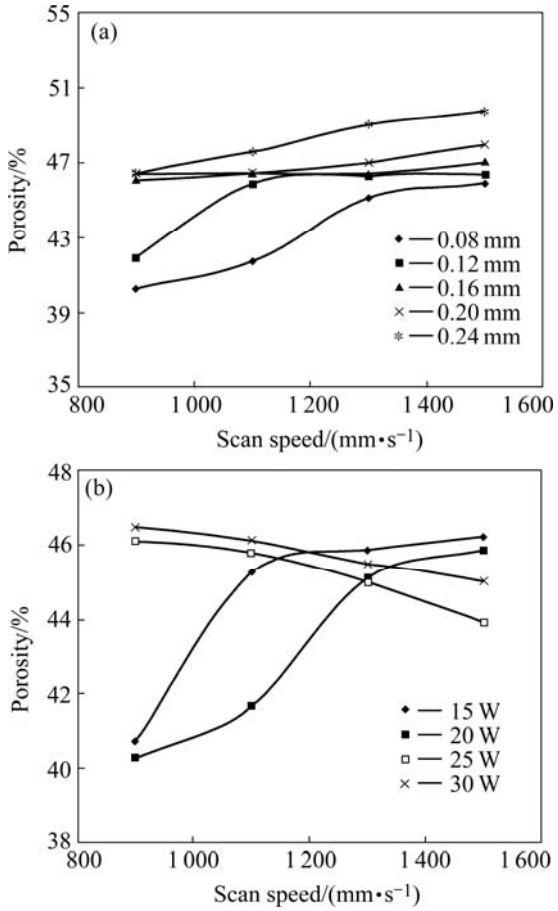

Fig.4 Effect of processing parameters on porosity of green sintered 316L stainless steel powder at constant laser power of 20 W (a) and constant scan spacing of 0.08 mm (b)

effect of scan speed on porosity at constant scan spacing. The porosity of the green parts reduces with increasing scan speed for high laser power (25 and 30 W) and at low laser power (15 and 20 W) the porosity of the green parts increases rapidly with increasing scan speed to 1 300 mm/s, and then increases slightly to 1 500 mm/s. Fig.5 shows the effect of laser power on the porosity at different scan speeds and constant scan spacing. It can be noticed that the density of the green parts depends on not only laser power and scan speed, but also scan spacing. It can, therefore, be concluded that intensifying the laser energy input (increasing laser power, decreasing scan

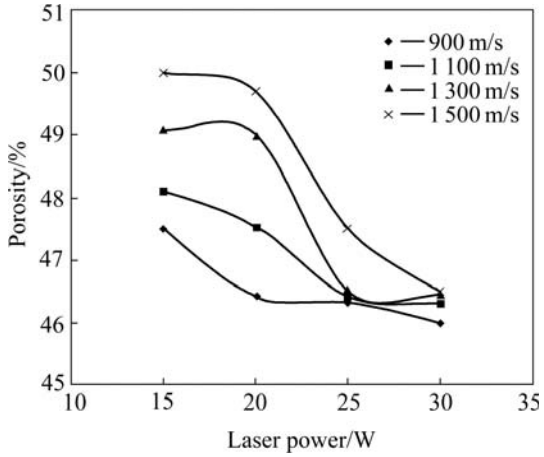

Fig.5 Effect of laser power on porosity of green parts at different scan speeds and constant scan spacing 0.08 mm

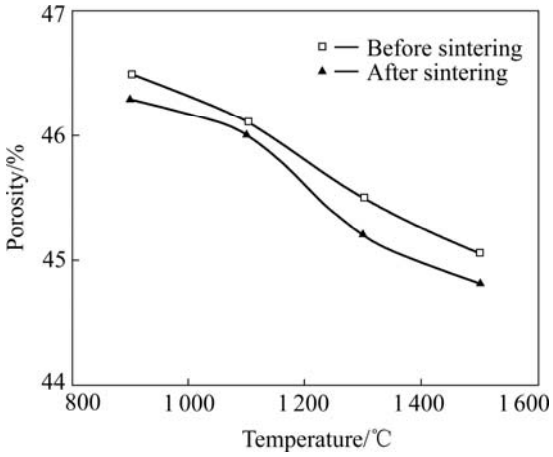

Fig.6 Effect of sintering cycle on porosity of 316L stainless steel for samples sintered at constant laser power (30 W) and constant scan spacing 0.08 mm

speed, and overlapping of scan lines) leads to higher densification for certain value. Further increase in energy intensity, (i.e., at high laser power, or slow scans speed, and/or small scan spacing) would cause a decrease in density (an increase of the porosity) of green parts. The increase in porosity is as a result of polymer degradation and expansion of the voids by trapped gases. The total energy intensity input (ψ) per unit area (J/mm^2) as a function of the processing parameters can be evaluated from[18]

$$\psi = P/(vh) \quad (1)$$

where P is the laser power, v is the scan speed, and h is the scan spacing. The density of the green laser sintered part is the average of the density of each sintered layer. So, it can be deemed that the energy input is in direct relation to the final density. The results show that there is a maximum density of the green parts (60% of theoretical density) at 0.205 J/mm^2, with a possible decreasing after that. The minimum density (i.e. maximum porosity) of green parts was found to be around 50%. Many attempts to manufacture parts with porosity higher than 50%, by using low laser power, high scan speed, and big scan spacing, were done but all of these attempts were failed due to the fragility of the green parts. Furthermore, the strength of the green part was too low to handle and put in the furnace for debinding and sintering cycle.

Fig.6 shows the effect of sintering cycle at laser power (30 W) and constant scan spacing on the porosity. It was found that sintering at 1 150 ℃ resulted in a slight higher density (lower porosity) than the green density of the samples. Reducing the porosity was found to be less than 1% of green porosity for all samples. Reducing the porosity is due to the burning of the binder, and a small value of shrinkage that occurred during the sintering cycle.

Fig.7 shows the compressive stress—strain curves of 316L stainless steel samples fabricated by selective laser sintering process and subsequent traditional sintering with different porosities. The curves were generally characterized by three distinct regions: 1) stress rising linearly with strain at low stresses (elastic deformation); 2) a long deformation plateau stage with small increases of flow stress to large strain; 3) a densification stage where the flow stress rapidly increases. The corresponding strengths for the samples with porosities 40%, 46%, and 50% are 20, 25, and 32 MPa, respectively. Reducing the porosity from 50% to 46% leads to an increase in the stress by a factor about 1.25, and reducing the porosity from 50% to 40% leads to an increase in the stress by a factor around 1.66.

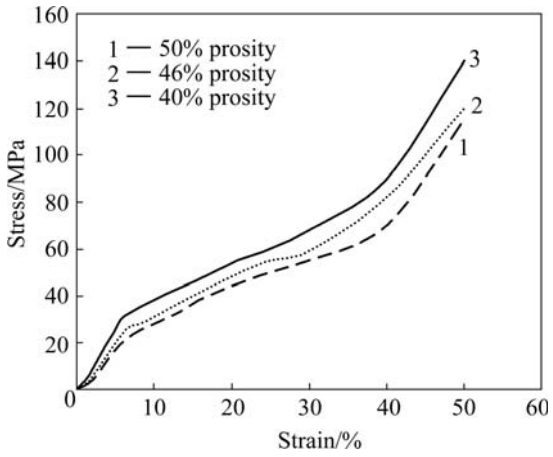

Fig.7 Compressive stress—strain curves of 316L stainless steel samples with different porosities

The mechanical properties of porous metals follow the model by GIBSON and ASHBY[19]. According to Gibson-Ashby model, the most important structural characteristic of a porous material that influences the

stress is its relative density ρ/ρ_s (the density of porous material (ρ) divided by that of the full solid material ρ_s). The relationship between the relative stress and relative density is given by

$$\frac{\sigma_{pl}}{\sigma_{ys}} = c\left(\frac{\rho}{\rho_s}\right)^{3/2} \quad (2)$$

where σ_{pl} is the stress of the porous part, σ_{ys} is the yield stress of the cell wall material and c is a constant. GIBSON and ASHBY[19] demonstrated that the value of c is 0.3 from the data of cellular metals and polymers. Nominal yield strength and the elastic modulus for fully dense 316L stainless steel is σ_{ys}=172 MPa and 193 GPa, respectively[20]. Fig.8 shows the effect of the porosity on the compressive strength of the porous 316L stain less steel parts fabricated by selective laser sintering and powder metallurgy. In this study, the stresses of the porous 316L stainless steel parts (40%, 46% and 50%) are approximately 20, 25, and 32 MPa. According to Eqn.(2), σ_{pl} of the present porous 316L stainless steel parts with porosities (40%, 46% and 50%) are 18.3, 20.5, and 24.0 MPa, respectively. It can be seen that the experimental data of stress is higher than the theoretical data. This higher stress in experimental is caused by the different deformation behavior between the theoretical hypothesis and the experimental[21].

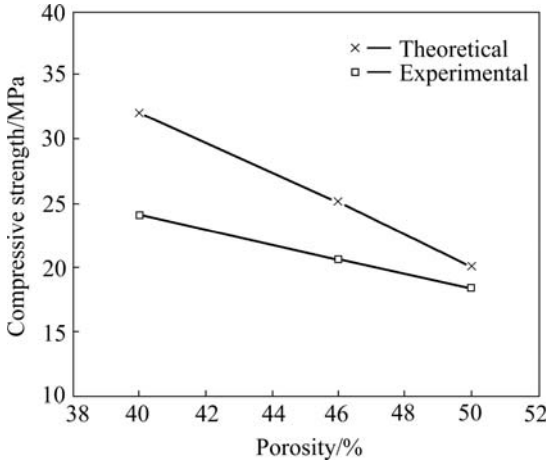

Fig.8 Compressive strength of sintered porous 316L stainless steel parts as function of porosity

Fig.9 shows the elastic modulus of the porous 316L stain less steel parts with different porosities. The elastic modulus increases with the decrease in porosity. The specimens with a low porosity of 40% show the high elastic modulus of 43 GPa. When the porosity increases from 40% to 50% the elastic modulus is only 26 GPa.

The microstructure of the samples is shown in Fig.10. Fig.10 indicates that powder bonding is achieved by neck growth through a solid-state diffusion process,

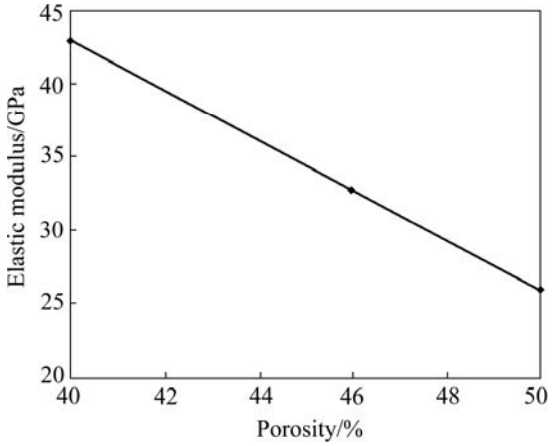

Fig.9 Elastic modulus of sintered porous 316L stainless steel parts as function of porosity

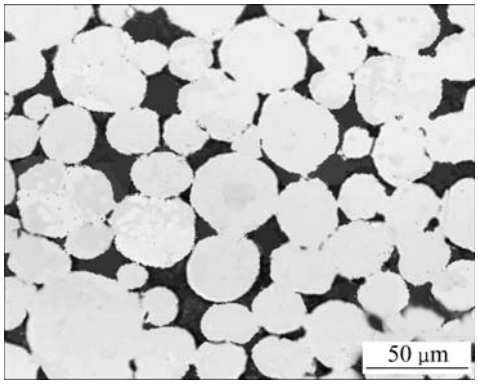

Fig.10 Microstructure of 316L stainless steel sample (after selective laser sintering process at scan speed 800 mm/s and laser power 20 W and post-sintering at 1 060 ℃ for 2 h) with porosity 29.5%

i.e., no liquid phase occurs. The shape of the pores is highly non-spherical, and the pores are cusped at sintering necks between powders.

4 Conclusions

1) Selective laser sintering allows the application of the traditional technique of powder metallurgy for the production of highly porous, near net shape 316L stainless steel.

2) Porous 316L stainless steel was successfully made by selective laser sintering process and traditional sintering. The porous 316L stainless steel made in such a way processes a porosity ranging from 40% to 50%. The compressive strength was found to be ranging from 21 to 32 MPa and corresponding elastic modulus ranging from 26 to 43 GPa.

3) Elastic modulus and compression strength of porous 316L parts having the porosity around 50% are close to those of human cortical bone.

4) Controlling the porosity of the material could be achieved by controlling the selective laser sintering parameters.

Acknowledgement

The research reported in this paper was supported by the Korea Research Foundation (KRF). The authors would like to thank the KRF for their support.

References

[1] LONG M, RACK H J. Titanium alloys in total joint replacement—A materials science perspective [J]. Biomaterials, 1998, 19: 1621−1639.

[2] BECKER B S, BOLTON J D. Corrosion behaviour and mechanical properties of functionally gradient materials developed for possible hard-tissue applications [J]. Journal of Materials Science: Materials in Medicine, 1997, 8: 793−797.

[3] LAPTEV A, BRAM M, BUCHKREMER H P, STOVER D. Study of production route for titanium parts combining very high porosity and complex shape [J]. Powder Metallurgy, 2004, 47(1): 85−92.

[4] THIEME M, WIETERS K P, BERGNER F, SCHARNWEBER D, WORCH H, NDOP J, KIM T J, GRILL W. Titanium powder sintering for preparation of a porous functionally graded material destined for orthopaedic implants [J]. Journal of Materials Science: Materials in Medicine, 2001, 12: 225−231.

[5] BAKAN H I. A novel water leaching and sintering process for manufacturing highly porous stainless steel [J]. Scripta Materialia, 2006, 55: 203−206.

[6] MANIATOPOULOS C, PILLIAR R M, SMITH D C. Threaded versus porous surfaced designs for implant stabilization in bone-endodontic implant model [J]. J Biomed Mater Res, 1986, 20(9): 1309−1333.

[7] MANIATOPOULOS C, PILLIAR R M, SMITH D C. Evaluation of shear strength at the cement-endodontic post interface [J]. J Prosthet Dent, 1988, 59(6): 662−669.

[8] MANIATOPOULOS C, PILLIAR R M, SMITH D C. Evaluation of the retention of endodontic implants [J]. J Prosthet Dent, 1988, 59(4): 438−446.

[9] SIMMONS C A, VALIQUETTE N, PILLIAR R M. Osseointegration of sintered porous-surfaced and plasma spray-coated implants: An animal model study of early post implantation healing response and mechanical stability [J]. J Biomed Mater Res, 1999, 47(2): 127−138.

[10] XIA Ren-long, LENG Yang, CHEN Ji-yong, ZHANG Qi-yi. A comparative study of calcium phosphate formation on bioceramics in vitro and in vivo [J]. Biomaterials, 2005, 26: 6477−6486.

[11] ANA Y B, OHA N H, CHUNA Y W, KIMA Y H, KIMA D K, PARKB J S, KWONC J J, CHOID K O, EOMD T G, BYUND T H, KIME J Y, REUCROFTF P J, KIMG K J, LEEA T W H. Mechanical properties of environmental-electro-discharge-sintered porous Ti implants [J]. Materials Letters, 2005, 59: 2178−2182.

[12] DENG X, PIOTROWSKI G B, WILLIAMS J J, CHAWLA N. Effect of porosity and tension-compression asymmetry on the Bauschinger effect in porous sintered steels [J]. International Journal of Fatigue, 2005, 27(10/12): 1233−1243.

[13] LEE W H, HYUN C Y. XPS study of porous dental implants fabricated by electro-discharge-sintering of spherical Ti-6Al-4V powders in a vacuum atmosphere [J]. Applied Surface Science, 2005, 353: 4250−4256.

[14] SUN Z M, MURUGAIAH A, ZHEN T, ZHOU Z, BARSOUM M W. Microstructure and mechanical properties of porous Ti_3SiC_2 [J]. Acta Materialia, 2005, 53: 4359−4366.

[15] WEN C E, YAMADA Y, SHIMOJIMA K, CHINO Y, ASAHINA T, MABUCHI M. Processing and mechanical properties of autogenous titanium implant materials [J]. Journal of Materials: Materials in Medical, 2002, 12: 397−401.

[16] GERMAN R M. Powder Metallurgy of Iron and Steel [M]. New York: John Wiley & Sons, Inc., 1998.

[17] DTM. Guide to Materials: RapidSteel^{TM} 2.0 Used to Produce Rapid Tool LR Mold Inserts DTM Corporation, DCN: 8002-10001, August, 1998.

[18] CAULFIELD B, MCHUGH P E, LOHFELD S. Dependence of mechanical properties of polyamide components on build parameters in the SLS process [J]. Journal of Materials Processing Technology, 2007, 182: 477−488.

[19] GIBSON L J, ASHBY M F. Cellular Solids: Structure and Properties [M]. Cambridge: Cambridge University Press, 1997.

[20] SCHADE C T, SCHABERL J. Development of stainless steel and high-alloy powders [C]//Advances in Powder Metallurgy and Particulate Materials. Princeton, NJ: Powder Industries Federation, 2004, 2: 148−153.

[21] WEN C E, MABUCHI M, YAMADA Y, SHIMOJIMA K, CHINO Y, ASAHINA T. Processing of biocompatible porous Ti and Mg [J]. Scripta Materialia, 2001, 45(10): 1147−1153.

(Edited by YANG Hua)